
Article:
Dedrick, James Peter orcid.org/0000-0003-4353-104X, Schröter, Sandra orcid.org/0000-0003-1029-4041, Niemi, Kari orcid.org/0000-0001-6134-1974 et al. (7 more authors) (2017) Controlled production of atomic oxygen and nitrogen in a pulsed radio-frequency atmospheric-pressure plasma. Journal of Physics D: Applied Physics. 455204. pp. 1-7. ISSN 1361-6463

https://doi.org/10.1088/1361-6463/aa8da2

Controlled production of atomic oxygen and nitrogen in a pulsed radio-frequency atmospheric-pressure plasma

J Dedrick[1,*], S Schröter[1], K Niemi[1], A Wijaikhum[1], E Wagenaars[1], N de Oliveira[2], L Nahon[2], J P Booth[3], D O'Connell[1], and T Gans[1]

[1] *York Plasma Institute, Department of Physics, University of York, Heslington YO10 5DD, York, UK*

[2] *Synchrotron Soleil, l'Orme des Merisiers, St. Aubin BP 48, 91192 Gif sur Yvette Cedex, France*

[3] *Laboratoire de Physique des plasmas, CNRS, École Polytechnique, UPMC Univ. Paris 06, Univ. Paris-Sud, Observatoire de Paris, Université Paris-Saclay, Sorbonne Universités, PSL Research University, F-91128 Palaiseau, France*

[*] *james.dedrick@york.ac.uk*

Abstract

Radio-frequency driven atmospheric pressure plasmas are efficient sources for the production of reactive species at ambient pressure and close to room temperature. Pulsing the radio-frequency power input provides additional control over species production and gas temperature. Here, we demonstrate the controlled production of highly reactive atomic oxygen and nitrogen in a pulsed radio-frequency (13.56 MHz) atmospheric-pressure plasma, operated with a small 0.1 % air-like admixture (N_2/O_2 at 4 : 1) through variations in the duty cycle. Absolute densities of atomic oxygen and nitrogen are determined through vacuum-ultraviolet absorption spectroscopy using the DESIRS beamline at the SOLEIL synchrotron coupled with a high resolution Fourier-transform spectrometer. The neutral-gas temperature is measured using nitrogen molecular optical emission spectroscopy. For a fixed applied-voltage amplitude (234 V), varying the pulse duty cycle from 10 % to 100 % at a fixed 10 kHz pulse frequency enables us to regulate the densities of atomic oxygen and nitrogen over the ranges of (0.18 ± 0.03) - $(3.7 \pm 0.1) \times 10^{20}$ m^{-3} and (0.2 ± 0.06) - $(4.4 \pm 0.8) \times 10^{19}$ m^{-3}, respectively. The corresponding 11 K increase in the neutral-gas temperature with increased duty cycle, up to a maximum of (314 ± 4) K, is relatively small. This additional degree of control, achieved through regulation of the pulse duty cycle and time-averaged power, could be of particular interest for prospective biomedical applications.

1 Introduction

Non-thermal atmospheric-pressure plasma jets (APPJs) enable efficient, non-aqueous delivery of chemically reactive species to temperature-sensitive materials[1]. Prospective applications in materials processing include the surface modification of polymers[2,3] and photoresist removal[4], and substantial progress has also been made with respect to a variety of biomedical applications[5,6], such as cancer therapy[7] and antimicrobial treatments[8]. A key feature is the capability to efficiently generate highly reactive neutral particles, including atomic oxygen and nitrogen, which are important to the surface interaction that occurs during material processing and also as precursors to longer-lived solvated reactive species that can play a key role in biological systems[9,10].

Low-voltage ($\backsim$hundreds of Volts) radio-frequency (rf, $\backsim$tens of MHz) APPJs are typically operated with a feed gas of helium (selected to minimise thermal instabilities through its relatively high thermal conductivity) with a small molecular admixture of oxygen and nitrogen (in the order of $\backsim$ 0.1 - 1%) to produce a spatially homogeneous discharge and reproducible fluxes of reactive species including atomic oxygen and nitrogen. Their stable operating range, between ignition and an uncontrolled constricted mode, typically spans about an order of magnitude in terms of the rf power dissipated in the plasma[11]. There is therefore a limited range of power that can be dissipated in the plasma, which limits the control over reactive species production and the neutral-gas temperature.

Enhanced control of time-averaged power dissipation is highly desirable, in particular for temperature sensitive applications such as biomedical technologies. Pulse modulation ($\backsim$kHz) techniques have proven to be very useful strategies for

low pressure rf plasmas and are broadly applied in industrial applications[12–14]. They have also been investigated at atmospheric pressure[15–20], and specifically to plasma sources that generate reactive species. Results to date, which have focused upon plasma sources operating with pure helium or helium-oxygen gas mixtures in the plasma core, highlight the promise of pulse modulation techniques for achieving additional control over reactive species production and the neutral-gas temperature, and in particular for enabling stable discharge operation at low average powers[21–25].

Gas mixtures that include oxygen and nitrogen, in particular those using an air-like ratio of 4:1, are especially important for applications requiring the production of reactive oxygen and nitrogen species in ambient air, for example biomedical technologies. Atomic oxygen and nitrogen have been shown to play key roles in the chemical kinetics of these systems[26–31]. In this study, we have therefore combined the use of rf pulse modulation with an air-like admixture (0.1 % N_2/O_2 at 4:1) to a helium-fed APPJ to more closely match the conditions of prospective applications.

In contrast to one-photon and two-photon laser induced fluorescence, which are widely used for the measurement of atomic species densities, absorption spectroscopy is insensitive to quenching. It is therefore well suited to the highly collisional conditions and complex gas mixtures that are most relevant to applications in ambient air. The time-honoured technique of resonance absorption spectroscopy has previously been applied in the experimentally challenging vacuum-ultraviolet (VUV) wavelength range for absolute density measurements of atomic oxygen and nitrogen in low-pressure plasmas[32–36]. It has also recently enabled the direct and absolute measurement of these densities in atmospheric-pressure plas-

mas using synchrotron radiation with a high-resolution Fourier-transform spectrometer[37]. This technique is experimentally complex and limited to specialised plasma sources that provide high vacuum compatibility. While it is important to note that absorption measurements are spatially integrated and are hence unable to detect the influence of spatial gradients across the beam cross-section and absorption length, the results of previous investigations combining experiments and simulations suggest that the atomic oxygen density remains relatively flat between the electrodes[26]. Here, we use this technique to quantify the influence of pulse modulation on the densities of atomic oxygen and nitrogen.

2 Experimental setup

Experiments are undertaken using the plasma source shown in Figure 1.

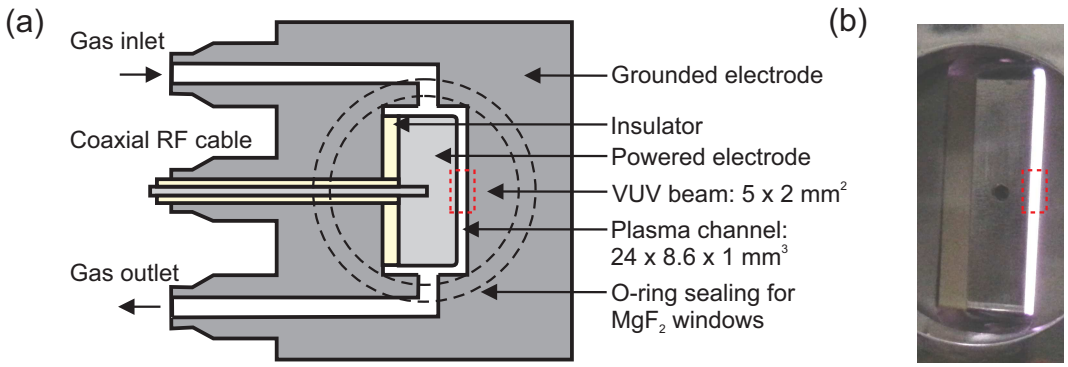

Figure 1: (a) Schematic cross-section and (b) photograph of the plasma source: The perpendicular orientation of the synchrotron vacuum ultraviolet (VUV) beam with respect to the plasma channel is indicated by the dashed rectangle.

This plasma source was designed to operate within the DESIRS (*Dichroïsme Et Spectroscopie par Interaction avec le Rayonnement Synchrotron*) beamline[38] at the SOLEIL synchrotron facility. The coupling of the VUV DESIRS beamline and

a unique Fourier transform spectrometer (VUV-FTS)[39] simultaneously enables high spectral resolution (resolving power $\lambda/\Delta\lambda$ up to $\approx 1 \times 10^6$) and broadband coverage over the full VUV spectral range[40].

The electrode material (stainless steel), length (24 mm) and spacing (1 mm) are selected to approach that of the well-characterised COST reference microplasma (μAPPJ) that operates in ambient air[41]. For vacuum compatibility, the electrode width is 8.6 mm and hence the surface-to-volume ratio of the channel (2.2 mm^{-1}) is smaller than that of the μAPPJ (4 mm^{-1}). To contain the gas within the vacuum chamber while allowing optical access, MgF_2 windows (1 mm thick) are installed on either side of the channel.

RF power at 13.56 MHz is coupled to the powered electrode using an arbitrary waveform generator (Tabor WS8352, 350 MHz), broadband amplifier (IFI SCCX100, 220 MHz) and matching network (Coaxial Power Systems MMN150). The housing of the plasma source forms the other electrode and is electrically grounded. For continuous operation, 9 W is coupled (amplifier reading: forward minus reflected power) to generate a homogeneous-glow-like α-mode discharge. This is lower than the 115 W applied in the previous measurement campaign of Ref. 37, and is a result of improved coupling efficiency and reduced flow of air-like admixture (N_2/O_2 at 4:1) to the 10 slm helium feed gas. The plasma properties are however considered to be comparable, as confirmed using measurements of the atomic oxygen and nitrogen densities for continuous power coupling to be described later. Here, an admixture of 0.1 % is used (on the low end of typical admixtures in these types of plasmas), which requires less rf power due to lower molecular dissociation, and minimizes neutral-gas heating at the same time.

A high-voltage probe (PMK, 14 KV_{rms}, 100 MHz) and oscilloscope (Lecroy Wave-

jet 354A, 500 MHz) are used to measure the applied voltage. The peak voltage amplitude is held constant at 234 V as shown in Figure 2. The pulse rise-time and fall-time, which are defined as the time for the voltage to increase or decrease between 10-90 % of its peak value (excluding overshoot), are 2.4 μs and 3.1 μs, respectively.

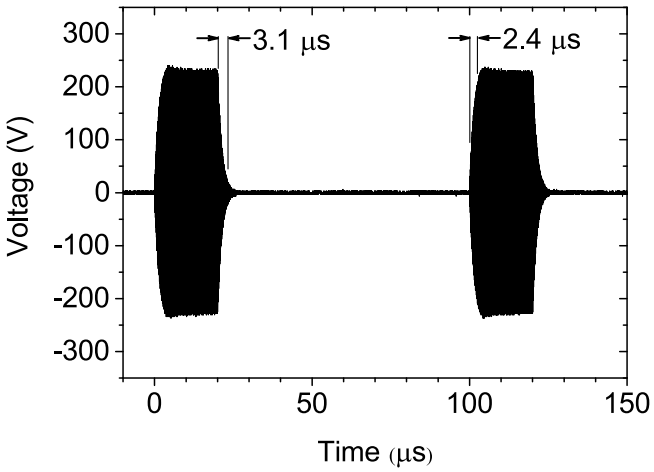

Figure 2: Representative rf voltage pulses applied to the plasma channel: 10 kHz modulation frequency with a duty cycle of 20 %. Helium flux 10 slm, N_2/O_2 (4:1) admixture 0.1 %.

To investigate the impact of pulse modulation on the production of atomic oxygen and nitrogen, two cases are considered: (1) variation of the pulse duty cycle over 10 - 100 % at a fixed modulation frequency of 10 kHz, and (2) variation of the pulse-modulation frequency over 1 - 50 kHz at a fixed duty cycle of 50 %.

To measure changes in gas heating, the neutral-gas temperature is determined using nitrogen molecular optical emission spectroscopy. A Czerny-Turner spectrograph (Andor SR500i, 0.5 m focal length, 2400 grooves/mm) with an attached non-intensified charge coupled device camera (Andor Newton DU940P-BU2, 2048×512 array of 13.5 μm^2 pixels) is used to measure the optical emission spectrum of the N_2

second-positive system ($C\ ^3\Pi \rightarrow B\ ^3\Pi$, $\nu = 0 \rightarrow 2$). Simulated spectra are fitted to the measurements to determine the gas temperature, by assuming that the rotational distribution is in thermal equilibrium with the neutral-gas temperature[42,43] as previously undertaken in high-pressure discharges for applications including, e.g. combustion[44], electric propulsion[45] and biomedicine[46–48]. Our spectrum simulation is based on molecular constants from Ref. 49 and line strength expressions from Ref. 50 for intermediate coupling of upper and lower state between Hund's case (a) and (b). The first rotational lines are treated according to Ref. 51, and Lambda-doubling is omitted. A Gaussian apparatus function is used in the analysis, and the spectral fitting routine is estimated to be accurate within ±4 K. However, results of the overall diagnostic technique should be treated conservatively[43] and for these conditions we consider the overall systematic uncertainty to be ±10 K.

Absolute densities of atomic oxygen and nitrogen, spatially averaged over the 1 mm electrode gap at the longitudinal midpoint of the plasma channel (VUV beam cross-section $\backsim 5 \times 2$ mm^2), are determined using VUV-FTS transmission spectra as described in Ref. 37. The O-atom and N-atom Doppler widths are $\Delta\sigma^{\mathrm{O}}{}_{\mathrm{D}}(308\ \mathrm{K}) = 0.24\ \mathrm{cm}^{-1}$ and $\Delta\sigma^{\mathrm{N}}{}_{\mathrm{D}}(308\ \mathrm{K}) = 0.28\ \mathrm{cm}^{-1}$, respectively, for a neutral-gas temperature of 308 K, representing the mean value found across all of our measurements. Representative transmission spectra for atomic oxygen and nitrogen are shown in Figure 3 and Figure 4, respectively, for a 10 kHz pulse-modulation frequency and duty cycle of 20 %.

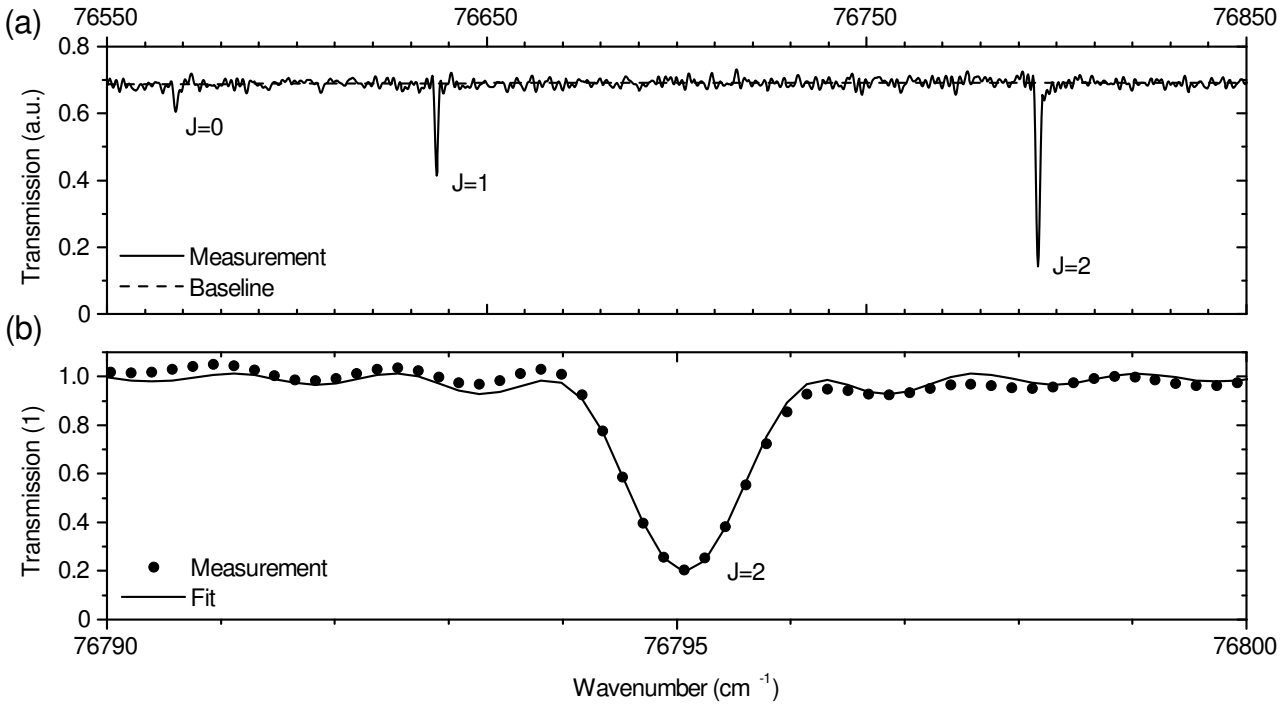

Figure 3: (a) Measured spectrum (not normalized or deconvoluted) and (b) normalized spectrum ($J = 2$ component) used to determine the density of atomic oxygen, $O(2p^4\ ^3P_J \rightarrow 3s\ ^3S^*_1)$. Helium flux 10 slm, N_2/O_2 (4:1) admixture 0.1 %, pulse voltage 234 V, pulse duty cycle 20 %, pulse frequency 10 kHz.

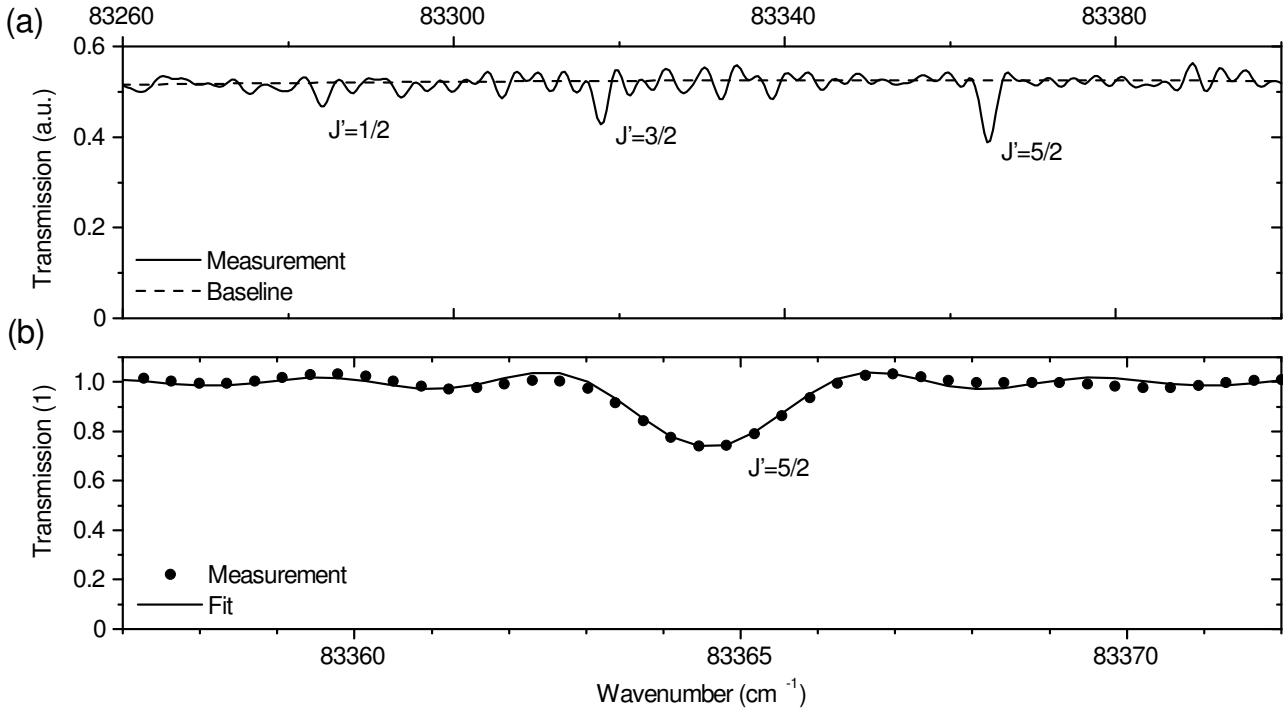

Figure 4: (a) Measured spectrum (not normalized or deconvoluted) and (b) normalized spectrum ($J^{'} = 5/2$ component) used to determine the density of atomic nitrogen, $N(2p^3\ ^4S^*_{3/2} \rightarrow 3s\ ^4P_{J'})$. Helium flux 10 slm, N_2/O_2 (4:1) admixture 0.1 %, pulse voltage 234 V, pulse duty cycle 20 %, pulse frequency 10 kHz.

3 Results

The variation of the atomic oxygen and nitrogen densities and neutral-gas temperature are shown in Figure 5 as a function of the pulse duty cycle. To confirm repeatability, two measurements were undertaken for the atomic oxygen density at a representative duty cycle of 20 %. Similarly, the density of atomic nitrogen was measured three times at a duty cycle of 90 %. The displayed data points represent average values. It is important to note that the expected decay time of the atomic densities, previously observed to be $\backsim$ms[26,31], is significantly longer than the time interval between pulses.

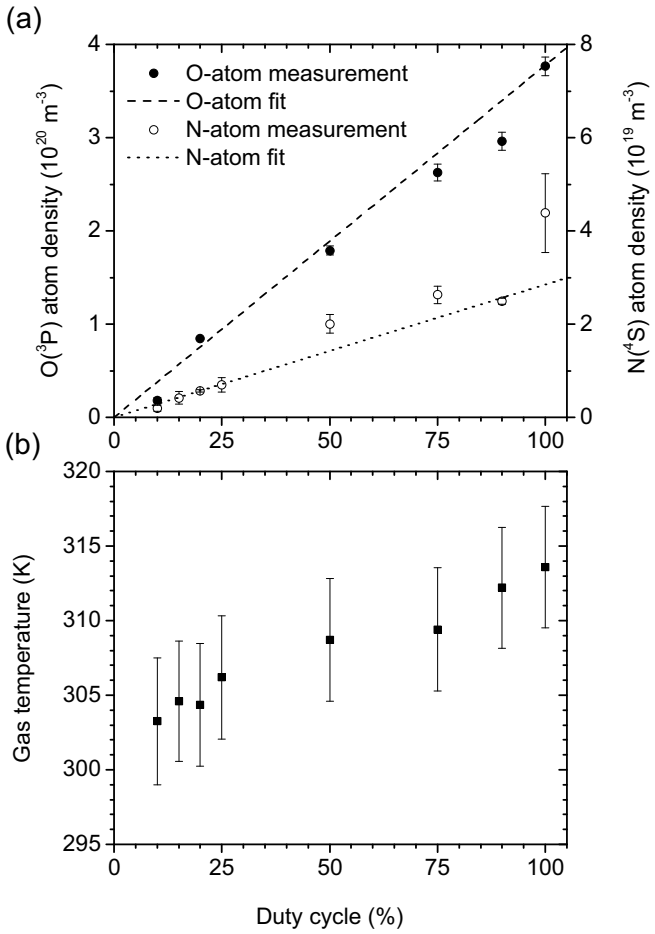

Figure 5: (a) Densities of atomic oxygen and atomic nitrogen, and (b) neutral-gas temperature with respect to pulse duty cycle. Helium flux 10 slm, N_2/O_2 (4:1) admixture 0.1 %, pulse voltage 234 V, pulse frequency 10 kHz.

The densities of atomic oxygen and nitrogen, shown in Figure 5 (a), were first measured for continuous power coupling (100 % duty cycle). They are observed to agree reasonably well (17 % increase and 23 % decrease, respectively) with that of Ref. 37 for the same gas mixture and low power, homogeneous-glow-like α-mode of operation.

In our previous investigation using continuous power coupling, we observed the densities of atomic oxygen and nitrogen to be maximal at 0.35 % and 0.1 % dry-

air admixture, respectively[37]. Therefore, in this work at a dry-air admixture of 0.1 %, we operate the source under a condition of maximal production of atomic nitrogen, while the maximal production of atomic oxygen is expected to occur at a slightly higher dry-air admixture.

When the plasma is pulsed, the densities of atomic oxygen and nitrogen are observed to increase linearly with duty cycle, varying between (0.18 ± 0.03) - $(3.7 \pm 0.1) \times 10^{20}$ m^{-3} and (0.2 ± 0.06) - $(4.4 \pm 0.8) \times 10^{19}$ m^{-3}, respectively, for duty cycles of 10 - 100 %. A linear increase in both densities with respect to the pulse duty cycle is consistent with the linearly increasing time-averaged rf power. It is important to note that the control in atomic-species density can be achieved in addition to that obtainable by changing the on-phase power level (not undertaken here), extending the range down to lower fluxes while ensuring stable plasma operation. The neutral-gas temperature, shown in Figure 5 (b), also exhibits a linear increase with duty cycle, where the gas temperature is measured to vary from (303 ± 4) - (314 ± 4) K for duty cycles of 10 - 100 %. These values are of significant interest as they can be used to benchmark future plasma chemistry models that incorporate both oxygen and nitrogen species.

The results as the pulse-frequency is varied for a fixed duty cycle of 50 % are shown in Figure 6 for (a) densities of atomic oxygen and nitrogen and (b) neutral-gas temperature.

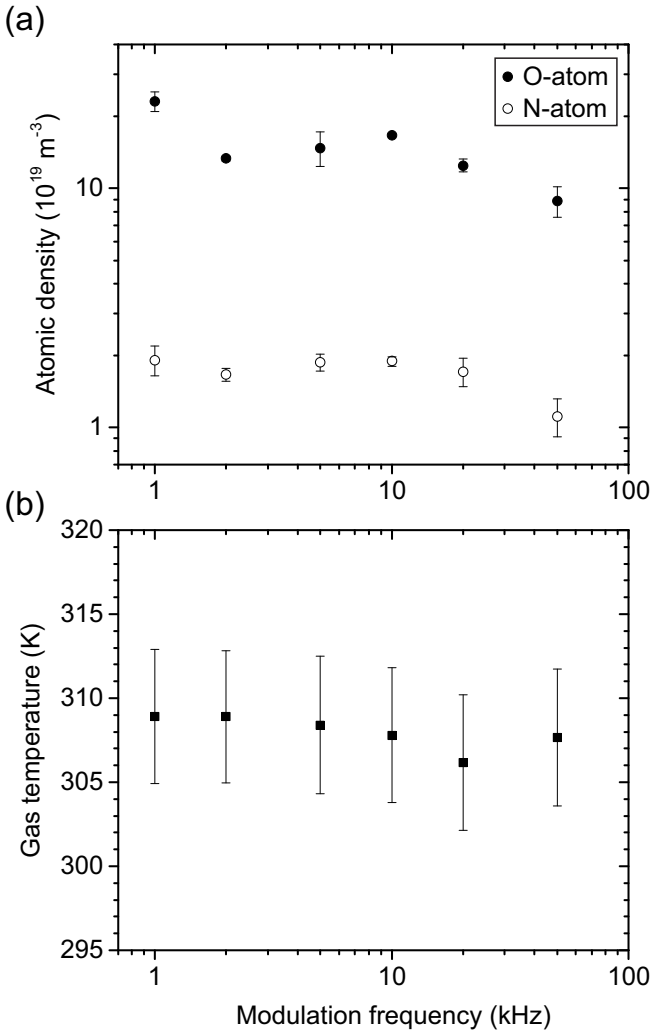

Figure 6: (a) Densities of atomic oxygen and atomic nitrogen, and (b) neutral-gas temperature with respect to pulse-modulation frequency. Helium flux 10 slm, N_2/O_2 (4:1) admixture 0.1 %, pulse voltage 234 V, pulse duty cycle 50 %.

In this case, the time-averaged power remains constant, independent of pulse frequency. Consistent with this, the neutral-gas temperature is observed to remain relatively constant for pulse frequencies of 1 - 50 kHz. The density of atomic oxygen is observed to be relatively independent of the pulse frequency, except above 20 kHz, where a small decrease is seen as shown in Figure 6 (a). This

agrees qualitatively with the results of recent fluid simulations of a capacitively coupled atmospheric-pressure plasma source (2 mm electrode separation) operating in helium with oxygen admixtures of 0 - 1 %[23].

The observed decrease in the atomic densities measured for a modulation frequency of 50 kHz could be attributed to the relatively large pulse rise-time compared to its duration (2.4 μs and 10 μs, respectively). However, as this is partially compensated by the pulse fall-time (3.1 μs) a more detailed experimental investigation of the temporal evolution in the afterglow remains the subject of future work.

4 Conclusion

The absolute densities of atomic oxygen and nitrogen have been measured in an rf-driven and pulse-modulated atmospheric-pressure plasma jet operating in helium with a small 0.1 % air-like admixture (N_2/O_2 at 4:1). The atomic densities were determined by vacuum-ultraviolet absorption spectroscopy using the DESIRS beamline at the SOLEIL synchrotron coupled with a high resolution Fourier-transform spectrometer. The neutral-gas temperature was measured using nitrogen molecular optical emission spectroscopy. The densities of atomic oxygen and nitrogen increase linearly with respect to pulse duty cycle, which is consistent with linear increases in the time-averaged power and neutral-gas temperature. Pulse modulation of the driving voltage enables stable operation of the discharge at lower average power compared to continuous operation, providing a lower neutral-gas temperature and densities of atomic oxygen and nitrogen. The direct and absolute measurement of reactive atomic species densities, without assumptions about

the ambient quenching conditions, provides valuable information for the ongoing development of plasma chemistry models. This will in-turn drive the development of experimental techniques for achieving enhanced precision in the production of reactive gas chemistry for prospective technological and biomedical applications.

Acknowledgements

The authors wish to thank J.-F. Gil and R. Armitage for their technical assistance at the DESIRS beamline and University of York, respectively. We are grateful to D. Joyeux for the development of the FTS and his help during the synchrotron campaign, together the general staff of SOLEIL for providing beam time under project 20130646. We also acknowledge financial assistance from EPSRC (EP/K018388/1 and EP/H003797/1), York-Paris Collaborative Research Centre, DPST scholarship from the Government of Thailand (A. Wijaikhum) and an Australian Government Endeavour Research Fellowship (J. Dedrick). This work was performed within the Plas@par project and received financial state aid by the "Agence Nationale de la Recherche", as part of the "Programme Investissements d'Avenir" under the reference ANR-11-IDEX-0004-02.

References

[1] M. Laroussi and T. Akan. Arc-free atmospheric pressure cold plasma jets: A review. *Plasma Processes and Polymers*, 4(9):777–788, 2007. ISSN 1612-8869. doi:10.1002/ppap.200700066.

[2] A. J. Knoll, P. Luan, E. A. J. Bartis, C. Hart, Y. Raitses, and G. S.

Oehrlein. Real time characterization of polymer surface modifications by an atmospheric-pressure plasma jet: Electrically coupled versus remote mode. *Applied Physics Letters*, 105(17):171601, 2014. doi:10.1063/1.4900551].

[3] D. Shaw, A. West, J. Bredin, and E. Wagenaars. Mechanisms behind surface modification of polypropylene film using an atmospheric-pressure plasma jet. *Plasma Sources Science and Technology*, 25(6):065018, 2016. doi:10.1088/0963-0252/25/6/065018.

[4] A. West, M. van der Schans, C. Xu, M. Cooke, and E. Wagenaars. Fast, downstream removal of photoresist using reactive oxygen species from the effluent of an atmospheric pressure plasma jet. *Plasma Sources Science and Technology*, 25(2):02LT01, 2016. doi:10.1088/0963-0252/25/2/02lt01.

[5] M. G. Kong, G. Kroesen, G. Morfill, T. Nosenko, T. Shimizu, J. van Dijk, and J. L. Zimmermann. Plasma medicine: an introductory review. *New Journal of Physics*, 11(11):115012, 2009. doi:10.1088/1367-2630/11/11/115012.

[6] Th. von Woedtke, S. Reuter, K. Masur, and K.-D. Weltmann. Plasmas for medicine. *Physics Reports*, 530(4):291–320, 2013. ISSN 0370-1573. doi:10.1016/j.physrep.2013.05.005.

[7] A. M. Hirst, M. S. Simms, V. M. Mann, N. J. Maitland, D. O'Connell, and F. M. Frame. Low-temperature plasma treatment induces DNA damage leading to necrotic cell death in primary prostate epithelial cells. *British Journal of Cancer*, 112(9):1536–1545, 2015. ISSN 1532-1827. doi:10.1038/bjc.2015.113.

[8] A. Privat-Maldonado, D. O'Connell, E. Welch, R. Vann, and M. W. van der Woude. Spatial dependence of DNA damage in bacteria due to low-

temperature plasma application as assessed at the single cell level. *Scientific Reports*, 6(35646), 2016. doi:10.1038/srep35646.

[9] D. B. Graves. The emerging role of reactive oxygen and nitrogen species in redox biology and some implications for plasma applications to medicine and biology. *Journal of Physics D: Applied Physics*, 45(26):263001, 2012. doi:10.1088/0022-3727/45/26/263001.

[10] A. Lindsay, C. Anderson, E. Slikboer, S. Shannon, and D. Graves. Momentum, heat, and neutral mass transport in convective atmospheric pressure plasma-liquid systems and implications for aqueous targets. *Journal of Physics D: Applied Physics*, 48(42):424007, 2015. doi:10.1088/0022-3727/48/42/424007.

[11] D. Marinov and N. St. J. Braithwaite. Power coupling and electrical characterization of a radio-frequency micro atmospheric pressure plasma jet. *Plasma Sources Science and Technology*, 23(6):062005, 2014. doi:10.1088/0963-0252/23/6/062005.

[12] T. Gans, M. Osiac, D. O'Connell, V. A. Kadetov, U. Czarnetzki, T. Schwarz-Selinger, H. Halfmann, and P. Awakowicz. Characterization of stationary and pulsed inductively coupled rf discharges for plasma sterilization. *Plasma Physics and Controlled Fusion*, 47(5A):A353, 2005. doi:10.1088/0741-3335/47/5A/026.

[13] M. Osiac, T. Schwarz-Selinger, D. O'Connell, B. Heil, Z. Lj. Petrovic, M. M. Turner, T. Gans, and U. Czarnetzki. Plasma boundary sheath in the afterglow of a pulsed inductively coupled rf plasma. *Plasma Sources Science and Technology*, 16(2):355, 2007. doi:10.1088/0963-0252/16/2/019.

[14] D. J. Economou. Pulsed plasma etching for semiconductor manufacturing. *Journal of Physics D: Applied Physics*, 47(30):303001, 2014. doi:10.1088/0022-3727/47/30/303001.

[15] J. J. Shi, J. Zhang, G. Qiu, J. L. Walsh, and M. G. Kong. Modes in a pulse-modulated radio-frequency dielectric-barrier glow discharge. *Applied Physics Letters*, 93(4):041502, 2008. doi:10.1063/1.2965453.

[16] J. Shi, Y. Cai, J. Zhang, and Y. Yang. Characteristics of pulse-modulated radio-frequency atmospheric pressure glow discharge. *Thin Solid Films*, 518 (3):962–966, 2009. doi:10.1016/j.tsf.2009.07.166.

[17] J. Shi, Y. Cai, J. Zhang, K. Ding, and J. Zhang. Discharge ignition characteristics of pulsed radio-frequency glow discharges in atmospheric helium. *Physics of Plasmas*, 16(7):070702, 2009. doi:10.1063/1.3184824.

[18] J. Sun, Q. Wang, Z. Ding, X. Li, and D. Wang. Numerical investigation of pulse-modulated atmospheric radio frequency discharges in helium under different duty cycles. *Physics of Plasmas*, 18(12):123502, 2011. doi:10.1063/1.3671967.

[19] X. Li, H. Wang, Z. Ding, and Y. Wang. Simulation of a pulse-modulated radio-frequency atmospheric pressure glow discharge. *Thin Solid Films*, 519 (20):6928–6930, 2011. doi:10.1016/j.tsf.2011.01.381.

[20] J. Dedrick, D. O'Connell, T. Gans, R. W. Boswell, and C. Charles. Formation of spatially periodic fronts of high-energy electrons in a radio-frequency driven surface microdischarge. *Applied Physics Letters*, 102(3):034109, 2013. ISSN 0003-6951. doi:10.1063/1.4789371.

[21] V. Leveille and S. Coulombe. Design and preliminary characterization of a miniature pulsed RF APGD torch with downstream injection of the source of reactive species. *Plasma Sources Science and Technology*, 14(3):467, 2005. doi:10.1088/0963-0252/14/3/008.

[22] D. L. Bayliss, J. L. Walsh, G. Shama, F. Iza, and M. G. Kong. Reduction and degradation of amyloid aggregates by a pulsed radio-frequency cold atmospheric plasma jet. *New Journal of Physics*, 11(11):115024, 2009. doi:10.1088/1367-2630/11/11/115024.

[23] Y.-T. Zhang, Y.-Y. Chi, and J. He. Numerical simulation on the production of reactive oxygen species in atmospheric pulse-modulated RF discharges with He/O_2 mixtures. *Plasma Processes and Polymers*, 11(7):639–646, 2014. doi:10.1002/ppap.201300200.

[24] K. McKay, J. L. Walsh, and J. W. Bradley. Observations of ionic species produced in an atmospheric pressure pulse-modulated RF plasma needle. *Plasma Sources Science and Technology*, 22(3):035005, 2013. doi:10.1088/0963-0252/22/3/035005.

[25] S. Kelly and M. M. Turner. Power modulation in an atmospheric pressure plasma jet. *Plasma Sources Science and Technology*, 23(6):065012, 2014. doi:10.1088/0963-0252/23/6/065012.

[26] J. Waskoenig, K. Niemi, N. Knake, L. M. Graham, S. Reuter, V. Schulz-von der Gathen, and T. Gans. Atomic oxygen formation in a radio-frequency driven micro-atmospheric pressure plasma jet. *Plasma Sources Science and Technology*, 19(4):045018, 2010. doi:10.1088/0963-0252/19/4/045018.

[27] E. Wagenaars, T. Gans, D. O'Connell, and K. Niemi. Two-photon absorption laser-induced fluorescence measurements of atomic nitrogen in a radio-frequency atmospheric-pressure plasma jet. *Plasma Sources Science and Technology*, 21(4):042002, 2012. ISSN 1361-6595. doi:10.1088/0963-0252/21/4/042002.

[28] D. Maletić, N. Puač, S. Lazović, G. Malović, T. Gans, V. Schulz-von der Gathen, and Z. Lj Petrović. Detection of atomic oxygen and nitrogen created in a radio-frequency-driven micro-scale atmospheric pressure plasma jet using mass spectrometry. *Plasma Physics and Controlled Fusion*, 54(12):124046, 2012. doi:10.1088/0741-3335/54/12/124046.

[29] T. Murakami, K. Niemi, T. Gans, D. O'Connell, and W. G. Graham. Chemical kinetics and reactive species in atmospheric pressure helium-oxygen plasmas with humid-air impurities. *Plasma Sources Science and Technology*, 22(1): 015003, 2013. doi:10.1088/0963-0252/22/1/015003.

[30] T. Murakami, K. Niemi, T. Gans, D. O'Connell, and W. G. Graham. Interacting kinetics of neutral and ionic species in an atmospheric-pressure helium–oxygen plasma with humid air impurities. *Plasma Sources Science and Technology*, 22(4):045010, 2013. doi:10.1088/0963-0252/22/4/045010.

[31] T. Murakami, K. Niemi, T. Gans, D. O'Connell, and W. G. Graham. Afterglow chemistry of atmospheric-pressure helium-oxygen plasmas with humid air impurity. *Plasma Sources Science and Technology*, 23(2):025005, 2014. doi:10.1088/0963-0252/23/2/025005.

[32] J. P. Booth, O. Joubert, J. Pelletier, and N. Sadeghi. Oxygen atom acti-

nometry reinvestigated: Comparison with absolute measurements by resonance absorption at 130 nm. *Journal of Applied Physics*, 69(2):618–626, 1991. doi:10.1063/1.347395.

[33] S. Takashima, M. Hori, T. Goto, A. Kono, M. Ito, and K. Yoneda. Vacuum ultraviolet absorption spectroscopy employing a microdiacharge hollow-cathode lamp for absolute density measurements of hydrogen atoms in reactive plasmas. *Applied Physics Letters*, 75(25):3929–3931, 1999. doi:10.1063/1.125497.

[34] S. Takashima, S. Arai, M. Hori, T. Goto, A. Kono, M. Ito, and K. Yoneda. Development of vacuum ultraviolet absorption spectroscopy technique employing nitrogen molecule microdischarge hollow cathode lamp for absolute density measurements of nitrogen atoms in process plasmas. *Journal of Vacuum Science & Technology A: Vacuum, Surfaces, and Films*, 19(2):599–602, 2001. doi:10.1116/1.1340655.

[35] H. Nagai, M. Hiramatsu, M. Hori, and T. Goto. Measurement of oxygen atom density employing vacuum ultraviolet absorption spectroscopy with microdischarge hollow cathode lamp. *Review of Scientific Instruments*, 74(7): 3453–3459, 2003. doi:10.1063/1.1582386.

[36] W. Takeuchi, H. Sasaki, S. Kato, S. Takashima, M. Hiramatsu, and M. Hori. Development of measurement technique for carbon atoms employing vacuum ultraviolet absorption spectroscopy with a microdischarge hollow-cathode lamp and its application to diagnostics of nanographene sheet material formation plasmas. *Journal of Applied Physics*, 105(11):113305, 2009. doi:10.1063/1.3091279.

[37] K. Niemi, D. O'Connell, N. de Oliveira, D. Joyeux, L. Nahon, J. P. Booth, and T. Gans. Absolute atomic oxygen and nitrogen densities in radio-frequency driven atmospheric pressure cold plasmas: Synchrotron vacuum ultra-violet high-resolution Fourier-transform absorption measurements. *Applied Physics Letters*, 103(3):034102, 2013. doi:10.1063/1.4813817.

[38] L. Nahon, N. de Oliveira, G. A. Garcia, J.-F. Gil, B. Pilette, O. Marcouillé, B. Lagarde, and F. Polack. DESIRS: a state-of-the-art VUV beamline featuring high resolution and variable polarization for spectroscopy and dichroism at SOLEIL. *Journal of Synchrotron Radiation*, 19(4):508–520, 2012. doi:10.1107/s0909049512010588.

[39] N. de Oliveira, D. Joyeux, M. Roudjane, J.-F. Gil, B. Pilette, L. Archer, K. Ito, and L. Nahon. The high-resolution absorption spectroscopy branch on the VUV beamline DESIRS at SOLEIL. *Journal of Synchrotron Radiation*, 23(4), 2016. doi:10.1107/S1600577516006135.

[40] N. de Oliveira, M. Roudjane, D. Joyeux, D. Phalippou, J.-C. Rodier, and L. Nahon. High-resolution broad-bandwidth Fourier-transform absorption spectroscopy in the VUV range down to 40 nm. *Nature Photonics*, 5(3): 149–153, 2011. ISSN 1749-4893. doi:10.1038/nphoton.2010.314.

[41] J. Golda, J. Held, B. Redeker, M. Konkowski, P. Beijer, A. Sobota, G. Kroesen, N. St. J. Braithwaite, S. Reuter, M. M. Turner, T. Gans, D. O'Connell, and V. Schulz-von der Gathen. Concepts and characteristics of the 'COST Reference Microplasma Jet'. *Journal of Physics D: Applied Physics*, 49(8): 084003, 2016. doi:10.1088/0022-3727/49/8/084003.

[42] U. Fantz. Basics of plasma spectroscopy. *Plasma Sources Science and Technology*, 15(4):S137–S147, Oct 2006. doi:10.1088/0963-0252/15/4/s01.

[43] P. J. Bruggeman, N. Sadeghi, D. C. Schram, and V. Linss. Gas temperature determination from rotational lines in non-equilibrium plasmas: a review. *Plasma Sources Science and Technology*, 23(2):023001, 2014. doi:10.1088/0963-0252/23/2/023001.

[44] M. S. Bak, W. Kim, and M. A. Cappelli. On the quenching of excited electronic states of molecular nitrogen in nanosecond pulsed discharges in atmospheric pressure air. *Applied Physics Letters*, 98(1):011502, 2011. doi:10.1063/1.3535986.

[45] A. Greig, C. Charles, R. Hawkins, and R. Boswell. Direct measurement of neutral gas heating in a radio-frequency electrothermal plasma micro-thruster. *Applied Physics Letters*, 103(7):074101, 2013. doi:10.1063/1.4818657.

[46] K. Niemi, S. Reuter, L. M. Graham, J. Waskoenig, N. Knake, V. Schulz-von der Gathen, and T. Gans. Diagnostic based modelling of radio-frequency driven atmospheric pressure plasmas. *Journal of Physics D: Applied Physics*, 43(12):124006, 2010. doi:10.1088/0022-3727/43/12/124006.

[47] T. Verreycken, A. F. H. Van Gessel, A. Pageau, and P. Bruggeman. Validation of gas temperature measurements by OES in an atmospheric air glow discharge with water electrode using Rayleigh scattering. *Plasma Sources Science and Technology*, 20(2):024002, 2011. doi:10.1088/0963-0252/20/2/024002.

[48] P. Bruggeman, G. Cunge, and N. Sadeghi. Absolute OH density measurements by broadband UV absorption in diffuse atmospheric-pressure He–H_2O RF

glow discharges. *Plasma Sources Science and Technology*, 21(3):035019, 2012. doi:10.1088/0963-0252/21/3/035019.

[49] F. Roux, F. Michaud, and M. Vervloet. High-resolution fourier spectrometry of $^{14}N_2$ violet emission spectrum: extensive analysis of the $C^3\Pi_u \rightarrow B^3\Pi_g$ system. *Journal of molecular spectroscopy*, 158(2):270–277, 1993. doi:10.1006/jmsp.1993.1071.

[50] I. Kovács. Formulae for rotational intensity distribution of triplet transitions in diatomic molecules. *The Astrophysical Journal*, 145:634–647, 1966. doi:10.1086/148802.

[51] A. Schadee. Theory of first rotational lines in transitions of diatomic molecules. *Astronomy and Astrophysics*, 41:203–212, 1975. URL http://adsabs.harvard.edu/abs/1975A%26A....41..203S.